Arch. Metall. Mater. **66** (2021), 4, 931-934

DOI: 10.24425/amm.2021.136399

HUIHUN KIM[1], MILAN K. SADAN[1], CHANGHYEON KIM[1], GA-IN CHOI[2], MINJUN SEONG[2], KWON-KOO CHO[2], KI-WON KIM[2], JOU-HYEON AHN[2], HYO-JUN AHN[1*]

ELECTROCHEMICAL PROPERTIES OF FLEXIBLE ANODE WITH SNO_2 NANOPOWDER FOR SODIUM-ION BATTERIES

Sodium-ion batteries (SIBs) have attracted substantial interest as an alternative to lithium-ion batteries because of the low cost. There have been many studies on the development of new anode materials that could react with sodium by conversion mechanism. SnO_2 is a promising candidate due to its low cost and high theoretical capacity. However, SnO_2 has the same problem as other anodes during the conversion reaction, i.e., the volume of the anode repeatedly expands and contracts by cycling. Herein, anode is composed of carbon nanofiber embedded with SnO_2 nanopowder. The resultant electrode showed improvement of cyclability. The optimized SnO_2 electrode showed high capacity of 1275 mAh g^{-1} at a current density of 50 mA g^{-1}. The high conductivity of the optimized electrode resulted in superior electrochemical performance.

Keywords: word, Sodium-ion batteries, SnO_2 anode, Flexible electrode, Nano SnO_2 particles, Ether based electrolyte

1. Introduction

Recently, in the energy research fields, the development of low-cost and large-scale batteries for electric vehicles and energy storage systems has become an urgent issue. Sodium-ion batteries (SIBs) are one of the most attractive alternatives to lithium-ion batteries because of the low cost and abundance of sodium [1,2]. The excellent performance of cathode materials for SIBs has already been reported [3,4]. Significant efforts also have been conducted on developing high-performance new anode materials for SIBs because graphite is not suitable for SIBs due to low specific capacity [5]. Thus, many studies have focused on the development of new anode materials that could react with sodium by phase conversion [6-8] or alloying [9-11] as those materials high theoretical capacity and electrical conductivity. SnO_2 is a promising candidate due to its low cost and high theoretical capacity [12]. However, SnO_2 has a problem during the conversion reaction. The volume of the product is higher than that of the initial materials, which results in volume variations lead to accumulation of internal stress, cracking, and finally pulverization into small particles [13]. This results in poor cyclability due to the disconnection between active materials and the current collector. To improve cycle life, previous research has focused on preventing pulverization through buffering volume changes by coating the SnO_2 with carbon materials [14-16]. However, these kinds of conducting materials reduce practical capacity. In addition, the practical capacity is more reduced through the addition of conducting agents, binders, and current collectors. Therefore, the addition of inactive materials such as conducting materials, binder, conducting agents, and current collector should be minimized [17,18].

In this work, we synthesis binder-free SnO_2 anode, which has a high degree of flexibility. In addition, by minimizing the current collector and conducting agents can improve electrode capacity. For higher electrochemical properties, the synthesis method was optimized by heating at various temperatures.

2. Experimental

2.1. Preparation of flexible SnO_2 anode

The SnO_2 anode was prepared by electrospun and heating PAN web mixed with SnO_2 nanopowder. The electrospinning solution was prepared by adding 2.46 g of polyacrylonitrile (PAN, Mw = 150,000, Sigma-Aldrich) and 1.5 g of SnO_2 nano-

[1] GYEONGSANG NATIONAL UNIVERSITY, RESEARCH INSTITUTE FOR GREEN ENERGY CONVERGENCE TECHNOLOGY, JINJU, 52828, REPUBLIC OF KOREA
[2] GYEONGSANG NATIONAL UNIVERSITY, DEPARTMENT OF MATERIALS ENGINEERING AND CONVERGENCE TECHNOLOGY, RIGET, JINJU, 52828, REPUBLIC OF KOREA
* Corresponding author: ahj@gnu.ac.kr

powder (Sigma-Aldrich) to 20 mL of *N*,*N*-dimethylformamaide (DMF, DAEJUNG, Korea). Then, the solution was homogeneously dispersed by ball milling (300 rpm) for 2 h and loaded into a 10-mL syringe with a metallic needle. The flow rate and positive voltage applied to the needle were 2 mL h^{-1} and 15 kV, respectively. After electrospinning, the as-spun PAN web with SnO_2 nanopowder was heated at a rate 5°C min^{-1} to 250°C for 3 h in air atmosphere for oxidative stabilization of PAN web. After oxidative stabilization, the sample was heated at a rate of 5°C min^{-1} to 400, 500, 700, and 1000°C and then maintained at this temperature for 3 h under an argon atmosphere. By heating, the PAN polymer web changed to a carbon nanofiber web. The various heating temperature was chosen due to the optimization of the synthesis condition of SnO_2 anode. The SnO_2 anode was punched into a 1 cm-diameter disc and directly used as an anode without any further processing.

2.2. Material characterization

The crystal structure of the samples was confirmed by XRD (D8 Advance A25, bruker), and their morphologies were examined by field-emission SEM (MIRA3 LM, TESCAN). The elemental contents of SnO_2 anode were determined using an elemental analyzer (EA, Vario Macro Cube, Elementar).

2.3. Electrochemical characterization

The SnO_2 anode was used as an anode without a conducting agent or binder. A Na foil was used as a counter electrode, and the separator was used a glass-fiber filter (GF/D, Whatman). 1M sodium hexafluorophosphate ($NaPF_6$, Sigma-Aldrich) in Dimethoxyethane (Sigma-Aldrich) was used as an electrolyte. The cell was assembled in a Swagelok-type cell in an argon-filled glove box. The discharge/charge tests were performed using a WBCS3000 battery cycler (WonATech, Korea) at room temperature. The specific capacity was calculated based on the weight of SnO_2.

3. Results and discussion

Fig. 1 shows photographic images of the SnO_2 electrodes after synthesis at various heating temperatures. Free-standing electrodes were obtained by heating a PAN web mixed with SnO_2 nanopowder. All free-standing SnO_2 electrodes web is foldable. Fig. 2 shows SEM images of the SnO_2 electrode. All SnO_2 electrode is composed of nanofiber with a diameter of several hundred nanometers and high aspect ratios. However, the particle size on the carbon nanofiber was different according to heating temperature. Below the heating temperature of 500°C, nanoparticles were observed. However, as the heating temperature increased, the particle size increased. Fig. 3 shows the XRD patterns of the SnO_2 electrode at various heating temperatures.

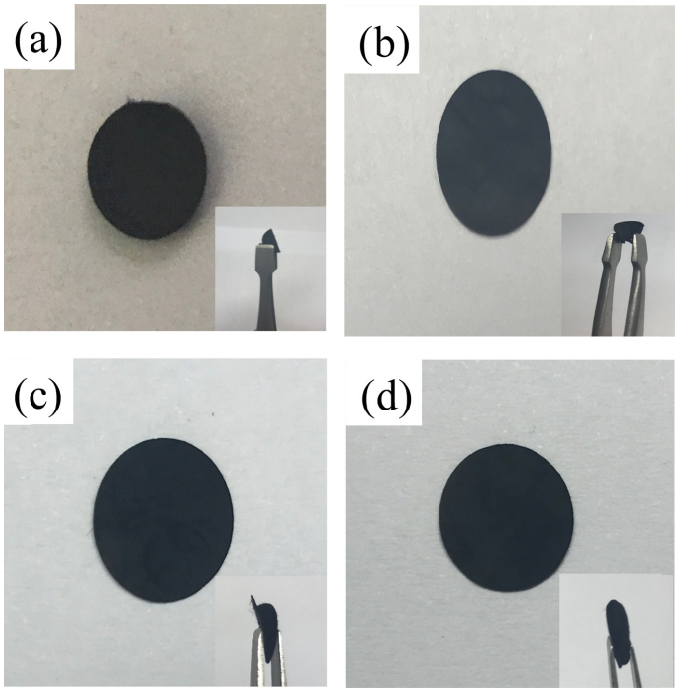

Fig. 1. The photograph of SnO_2 electrode according to different heat treatment temperature; (a) 400°C, (b) 500°C, (c) 700°C and (d) 1000°C

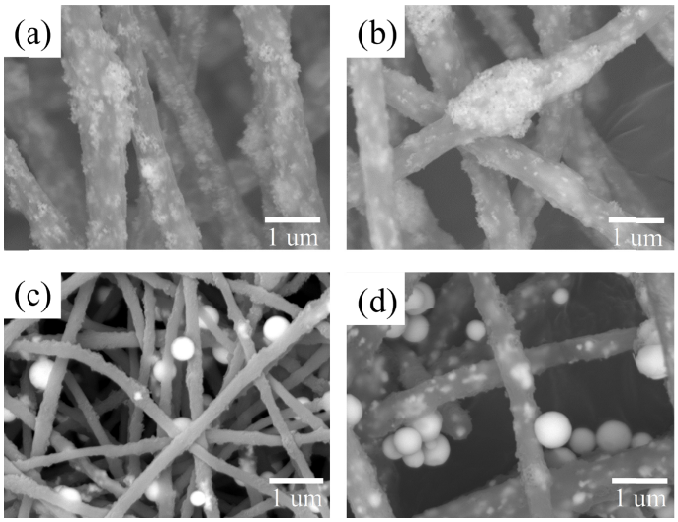

Fig. 2. FE-SEM images of electrodes with different heating temperature; (a) 400°C, (b) 500°C, (c) 700°C and (d) 1000°C

The structure of precursor SnO_2 nanopowder with PAN polymer web is tetragonal, and any other peaks were not observed. After oxidative stabilization, the crystal structure was maintained, which means that oxidative stabilization was not an effect of the phase of SnO_2 nanopowder. During the carbonization heating below 500°C, the tetragonal SnO_2 phase was maintained, which means that only PAN polymer was converted to carbon. However, the SnO_2 phase was disappeared and the cubic phase of Sn has appeared. On the high heating temperature, SnO_2 was reduced to Sn such as equation (1).

$$SnO_2 + C \rightarrow Sn + CO_2\uparrow \quad (1)$$

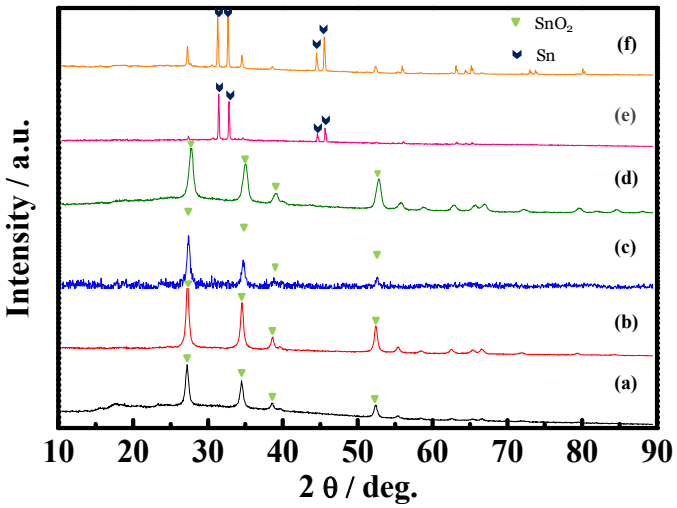

Fig. 3. XRD patterns of precursor and electrodes; (a) as-electrospun PAN with SnO_2 nanopowder and heat treated at (b) 250°C (oxidative stabilization), (c) 400°C, (d) 500°C, (e) 700°C and (f) 1000°C

We focused on SnO_2 anode except for Sn anode because SnO_2 particles were formed inside of carbon nanofiber, which can obtain buffer effect of carbon nanofiber during charge/discharge. In addition, smaller active materials size of SnO_2 was expected fast ion transfer.

In order to confirm the SnO_2 ratio in the electrode, the elemental analysis was analyzed. The 400°C and 500°C SnO_2 anode contain 41.2 and 44.8 wt % of SnO_2, respectively.

To determine the electrochemical performance of SnO_2 anode for SIBs, the Na/SnO_2 half-cell was tested using an ether-based electrolyte. Fig. 4 shows the cyclability of the SnO_2

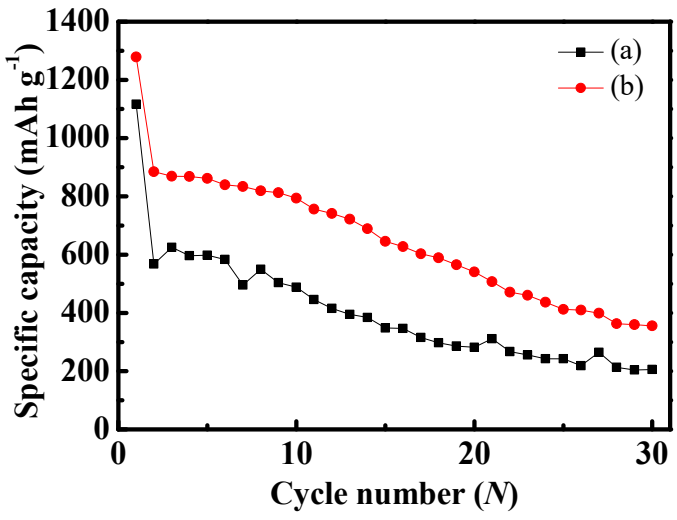

Fig. 4. The cycle performance of Na/SnO_2 cell at different heating temperature; (a) 400°C and (b) 500°C

anode at a current density of 50 mA g^{-1}. Between the first and second capacity has a high irreversible capacity which might be the formation of a solid electrolyte interfacial (SEI) layer [19-21]. The 2nd specific capacity of SnO_2 anode shows 871 and 556 mAh g^{-1} at heating temperature 500 and 400°C, respectively. The high specific capacity was due to as reported conversion reaction follow as [22]:

$$SnO_2 + 4Na^+ + 4e \leftrightarrow Sn + 2Na_2O \quad (2)$$

$$Sn + 2Na_2O + xNa^+ + xe^- \leftrightarrow Na_xSn + 2Na_2O \quad (3)$$

Therefore, the specific capacity after 30th cycles, the SnO_2 anode shows 360 (500°C) and 199 (400°C) mAh g^{-1}, respectively. The SnO_2 anode synthesized at 500°C shows superior cyclability than 400°C electrode. To understand the reason for the cyclability difference, we analyzed charge/discharge curves. Fig. 5 shows the 3rd charge/discharge curves of Na/SnO_2 cells. The sloping charge/discharge curves were observed and no clear plateau was found. The SnO_2 at 500°C has a smaller overpotential than SnO_2 at 400°C, which means that the resistance of SnO_2 at 500°C electrode was small. This small resistance might come from high heating temperature, which can improve the electric conductivity of carbon nanofiber. Chien group shows high electrical conductivity of the PAN fibers at the high heating temperature [23]. SnO_2 at 500°C electrode might have high electrical conductivity than SnO_2 at 400°C electrode. SnO_2 syntheized at high temperature has extended carbon structures, which increased conductivity of the electrode.

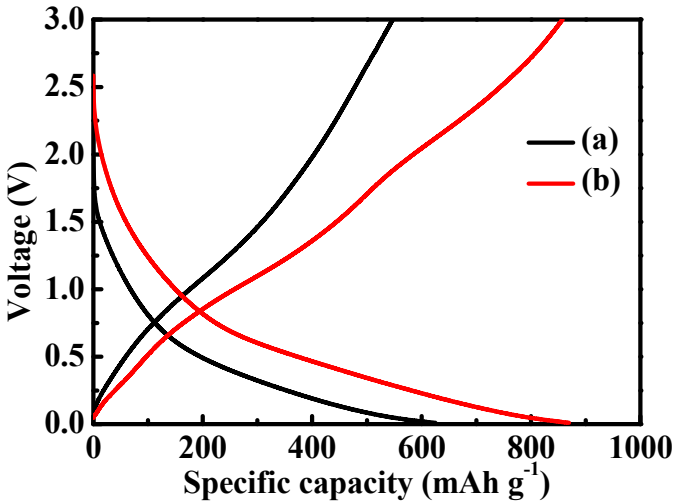

Fig. 5. The 3rd charge/discharge curves of Na/SnO_2 at different heating temperature; (a) 400°C and (b) 500°C

These results indicated the possibility for next-generation SIBs because of their high electrode capacity and flexibility. For practical application, it is necessary to further study the improved electric conductivity, which can obtain the novel flexible and high capacity anode for SIBs.

4. Conclusion

An anode of flexible and free-standing SnO_2 anode was prepared by electrospinning and heating. The optimized heating temperature was at 500°C, which has a high specific capacity and low resistance. The initial discharge capacity was 1275 mAh g^{-1},

but the 2nd discharge capacity was 871 mAh g^{-1}. The irreversible behavior might be related to SEI layer formation. In summary, the flexible SnO_2 anode is a candidate sodium-ion batteries anode material.

Acknowledgements

This work was supported by the project (2020R1A6A3A01100036, 2020R1A2C1101863, 2019H1D8A2105994) through the National Research Foundation of Korea (NRF)

REFERENCES

[1] L. Yue, H. Zhao, Z. Wu, J. Liang, S. Lu, G. Chen, S. Gao, B. Zhong, X. Guo, X. Sun, J. Mater. Chem. A. **8** (23), 11493-11510 (2020).

[2] K. Mishra, N. Yadav, S. Hashmi, J. Mater. Chem. A. **8** (43), 22507-22543 (2020).

[3] M.K. Sadan, A.K. Haridas, H. Kim, C. Kim, G.-B. Cho, K.-K. Cho, J.-H. Ahn, H.-J. Ahn, Nanoscale Advances. **2** (11), 5166-5170 (2020).

[4] M.K. Sadan, H. Kim, C. Kim, S. Cha, K.-K. Cho, K.-W. Kim, J.-H. Ahn, H.-J. Ahn, J. Mater. Chem. A. **8** (19), 9843-9849 (2020).

[5] Z. Zhu, F. Cheng, Z. Hu, Z. Niu, J. Chen, J. Power Sources. **293**, 626-634 (2015).

[6] H. Kim, M.K. Sadan, C. Kim, S.-H. Choe, K.-K. Cho, K.-W. Kim, J.-H. Ahn, H.-J. Ahn, J. Mater. Chem. A. **7** (27), 16239-16248 (2019).

[7] H. Kim, S.-W. Lee, K.-Y. Lee, J.-W. Park, H.-S. Ryu, K.-K. Cho, G.-B. Cho, K.-W. Kim, J.-H. Ahn, H.-J. Ahn, J. Nanosci. Nanotechnol. **18** (9), 6422-6426 (2018).

[8] H. Ye, L. Wang, S. Deng, X. Zeng, K. Nie, P.N. Duchesne, B. Wang, S. Liu, J. Zhou, F. Zhao, N. Han, P. Zhang, J. Zhong, X. Sun, Y. Li, Y. Li, J. Lu, Adv. Energy Mater. **7** (5), 1601602 (2016).

[9] C. Kim, I. Kim, H. Kim, M.K. Sadan, H. Yeo, G. Cho, J. Ahn, J. Ahn, H. Ahn, J. Mater. Chem. A. **6** (45), 22809-22818 (2018).

[10] M.K. Sadan, S.-H. Choi, H. Kim, C. Kim, G.-B. Cho, K.-W. Kim, N.S, Reddy, J.-H. Ahn, H.-J. Ahn, Ionics. **24**, 753-761 (2018).

[11] D. Su, S. Dou, G. Wang, Nano Energy. **12**, 88-95 (2015).

[12] D. Narsimulu, G. Nagaraju, S.C. Sekhar, B. Ramulu, J.S. Yu, Appl. Surf. Sci. **538**, 148033 (2021).

[13] L. Wang, J. Wang, F. Guo, L. Ma, Y. Ren, T. Wu, P. Zuo, G. Yin, J. Wang, Nano Energy. **43**, 184-191 (2018).

[14] S. Zhang, L. Yue, M. Wang, Y. Feng, Z. Li, J. Mi, Solid State Ion. **323**, 105-111 (2018).

[15] X. Lu, F. Luo, Q. Xiong, H. Chi, H. Qin, Z. Ji, L. Tong, H. Pan, Mater. Res. Bull. **99**, 45-51 (2018).

[16] Y.-N. Sun, M. Goktas, L. Zhao, P. Adelhelm, B.-H. Han, J. Colloid Interface Sci. **572**, 122-132 (2020).

[17] A.K. Haridas, J. Heo, X. Li, H.-J. Ahn, X. Zhao, Z. Deng, M. Agostini, A. Matic, J.-H. Ahn, Chem. Eng. J. **385**, 123453 (2020).

[18] M. K.Sadan, H. Kim, C. Kim, G.-B. Cho, N.S. Reddy, K.-K. Cho, T.-H. Nam, K.-W. Kim, J.-H. Ahn, H.-J. Ahn, J. Nanosci. Nanotechnol. **20** (11), 7119-7123 (2020).

[19] S. Men, H. Zheng, D. Ma, X. Huang, X. Kang, J. Energy Chem. **54**, 124-130 (2021).

[20] H. Xie, Z. Wu, Z. Wang, N. Qin, Y. Li, Y. Cao, Z. Lu, J. Mater. Chem. A. **8** (7), 3606-3612 (2020).

[21] G. Cha, S. Mohajernia, N.T. Nguyen, A. Mazare, N. Denisov, I. Hwang, P. Schmuki, Adv. Energy Mater. **10** (6), 1903448 (2020).

[22] Y.C. Lu, C. Ma, J. Alvarado, T. Kidera, N. Dimov, Y.S. Meng, S. Okada, J. Power Sources. **204**, 287-295 (2015).

[23] A.-T. Chien, S. Cho, Y. Joshi, S. Kumar, Polymer. **55** (26), 6896-6905 (2014).